AGU100 ADVANCING EARTH AND SPACE SCIENCE

Geophysical Research Letters

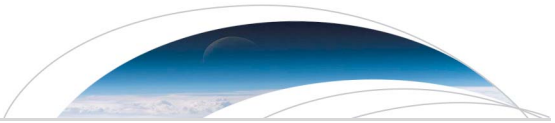

RESEARCH LETTER

10.1029/2018GL079598

Key Points:

- CFD data provide a more complete understanding of Martian sediment transport, augmenting ripple mapping studies
- Dune length scale modeling highlights areas of elevated surface shear stress that affect localized sediment flux
- Detailed seasonal 3-D airflow structures are presented that have not been previously attainable using mesoscale models

Supporting Information:

- Supporting Information S1
- Figure S1
- Figure S2
- Figure S3
- Figure S4
- Figure S5
- Figure S6
- Figure S7
- Figure S8
- Table S1

Correspondence to:
C. Cornwall,
cornwall-c@email.ulster.ac.uk

Citation:
Cornwall, C., Jackson, D. W. T., Bourke, M. C., Beyers, M., & Cooper, J. A. G. (2018). Seasonal variations in airflow over the Namib Dune, Gale Crater, Mars: Implications for dune dynamics. *Geophysical Research Letters*, *45*. https://doi.org/10.1029/2018GL079598

Received 12 JUL 2018
Accepted 6 SEP 2018
Accepted article online 11 SEP 2018

Seasonal Variations in Airflow Over the Namib Dune, Gale Crater, Mars: Implications for Dune Dynamics

Carin Cornwall[1], Derek W. T. Jackson[1], Mary C. Bourke[2], Meiring Beyers[3], and J. Andrew G. Cooper[1]

[1]Geography and Environmental Sciences, Ulster University, Coleraine, UK, [2]Geography, Trinity College, Dublin, Ireland, [3]Klimaat Consulting, Guelph, Ontario, Canada

Abstract Dune length scale airflow modeling provides new insights on eolian bedform response and complex near-surface 3-D wind patterns not previously resolved by mesoscale models. At a 1-m surface resolution, Curiosity wind data are used to investigate the eolian environment of the Namib dune on Mars, providing improved seasonal constraints on grainfall, grainflow activity, and ripple migration. Based on satellite images, airflow patterns, and surface shear stress, enhanced eolian activity, and slipface advancement occurs during early springtime. Autumn and winter winds are also favorable to eolian activity, but minimal movement was detected in satellite images overlapping with wind data. During the summer, the migration of large stoss ripples on the Namib dune may augment sediment deposition on the slipface. These results provide a better understanding of the overall migration pattern of the Namib dune, which can be extrapolated to other dunes in the Bagnold Dune Field.

Plain Language Summary At 1-m resolution, small-scale airflow modeling can provide new insights into sediment transport and dune migration on Mars. Coupled with wind data collected by the Curiosity rover, this study provides improved, realistic constraints on Martian sediment movement and illustrates how ripples seasonally form and migrate according to changing wind speeds and directions. The spring season with northerly winds is the most influential for dune migration based on modeling results and satellite monitoring, but the quieter summer and autumn seasons with southeasterly winds continue to facilitate ripple migration, which may help maintain slower rates of dune migration despite the opposing wind direction. Based on modeling results, the winter season with high-magnitude northerly winds should produce migration rates similar to spring, but according to satellite monitoring, dune migration stops. Small amounts of frost in between sand grains on the dune surface may be responsible for this halt in dune migration. These results can be applied to other dunes in the Bagnold Dune Field, which likely experience the same seasonal patterns in sediment transport.

1. Introduction

Curiosity Rover provided the first in situ observations and sediment analysis of Martian dunes while traversing the Bagnold Dune Field toward Aeolis Mons in Gale Crater (Figure S1). Images taken by Curiosity of the Namib dune slipface revealed a detailed record of grainflows, ripple formation, and tensional cracks (Cornwall, Bourke, et al., 2018; Ewing et al., 2017), similar to terrestrial dunes (Cornwall, Jackson, et al., 2018). The Bagnold dune field is active (Silvestro et al., 2013) but Curiosity visited the dunes during late autumn, a time of decreased eolian activity with little sediment movement (Bridges et al., 2017). The Martian atmospheric density and gravity are much lower than Earth, and therefore, wind speeds need to be 7 times greater to initiate grain saltation. However, once a grain is in motion, it can stay mobilized at a lower shear stress (Greeley et al., 1980; Greeley & Iversen, 1985; Kok, 2010a, 2010b; Kok et al., 2012; Kok & Renno, 2009). Based on terrestrial studies, grainflow formation requires an accumulation of sediment from grainfall, resulting in localized over-steepening, destabilization, and subsequent slope failure (e.g., Allen, 1970; Anderson, 1988; Hunter, 1985; McDonald & Anderson, 1995; Sutton et al., 2013). The preserved grainflows on the Namib dune slipface indicate that eolian conditions were favorable, at some point, to grainfall, but it is unclear precisely when grainfall occurred.

Airflow modeling research on Mars has focused largely on global patterns with general circulation models, which have provided a valuable foundation for understanding atmospheric-surface interactions (e.g., Fenton & Richardson, 2001; Greeley et al., 1993; Haberle et al., 1993; Hourdin & Forget, 1995; Leovy &

Mintz, 1969; Lee & Thomas, 1995; Richardson et al., 2007). However, dunes are heavily influenced by local wind patterns, unresolved by general circulation models, that shape morphology and control sediment transport (e.g., Fenton et al., 2005; Greeley et al., 1993, 2006; Hayward et al., 2007, 2008, 2009).

Mesoscale climate models, with a resolution of hundreds of meters, have achieved a more detailed study of local wind regimes, providing a regional context of short-timescale wind flow variability but are better suited for dune field airflow analysis (e.g., Fenton et al., 2005; Hobbs et al., 2010; Newman et al., 2017; Pla-Garcia et al., 2016; Rafkin et al., 2001, 2016; Richardson et al., 2007; Spiga & Forget, 2009; Toigo & Richardson, 2002; Tyler et al., 2002). Mesoscale models with bedform morphology analysis of the Bagnold Dune Field revealed a bimodal wind regime influenced by the crater floor topography with primary winds from the NW and secondary winds from the NE (Bridges et al., 2017; Day & Kocurek, 2016; Hobbs et al., 2010; Newman et al., 2017; Silvestro et al., 2013, 2016). Unfortunately, with model resolutions of ~500 m, forcing mechanisms that drive dune migration cannot be studied in full detail (Newman et al., 2017; Pla-Garcia et al., 2016; Rafkin et al., 2016), preventing a more comprehensive understanding of eolian processes operating in Gale Crater.

Analysis of eolian morphodynamics of individual dunes requires a spatial scale smaller than the dimensions of the dune to properly assess how local wind patterns affect eolian processes. Local topography can significantly influence wind speed and direction, thereby also affecting surface shear stress and enabling sediment transport during seasons of low magnitude winds. Eolian 2-D ripple mapping studies can offer some insights into surface airflow and sediment flux, but in areas absent of ripples, there is no information on airflow direction or magnitude modification, which can significantly impact dune morphology and create localized areas of greater surface shear stress. In addition, knowledge of detailed 3-D flow structures and turbulence is unattainable using mesoscale models or ripple mapping techniques.

Recent efforts have employed 3-D dune length scale computational fluid dynamics (CFD) modeling with a resolution <5 m to investigate these smaller airflow patterns and how they influence dune morphology and sediment transport (Jackson et al., 2015). This study uses a dune length scale CFD model with a High Resolution Imaging Science Experiment (HiRISE) Digital Terrain Model (DTM) of the Namib dune at a 1-m horizontal resolution, which adequately resolves subdune scale bedforms and provides a more comprehensive investigation of complex airflow patterns (Jackson et al., 2015). Seasonal results of dune length scale airflow modeling reveal complex, turbulent, and steered airflow on the dune slipface as well as in the immediate vicinity of the dune. An investigation of how these complex seasonal flow patterns may affect grainflow activity on the slipface and overall dune migration is presented for the Namib dune (−4.686°N, 222.364°W) using Mars Science Laboratory's (MSL) Curiosity Rover Environmental Monitoring Station (REMS) data (S2), a HiRISE DEM (S3), and the open source CFD software OpenFOAM (S4) to simulate the local Martian wind regime.

2. Results

The local wind regime in Gale Crater is complex, with a wide range of wind directions and magnitudes during a single Mars year (MY; Figure S1). REMS data in this study include MY 32 summer and MY 33 autumn, winter, and spring and indicates that the greatest magnitude near-surface winds predominantly originated from the north, agreeing with dune orientation and migration to the south. Lesser magnitude winds also occurred, and it appears that southerly winds may also have an impact on dune morphology and slipface processes.

2.1. Seasonal Patterns

2.1.1. Spring (L_s 180°)

Higher magnitude winds occurred early in the season, between Martian solar days ~1,400 and 1,430 and originated from the north (Figure 1) with an average wind velocity of 9.84 m/s (Table S4). The more predominant but lesser magnitude winds during the spring varied between east, southeast, and southwest (Figure 1). These secondary winds had an average wind speed of 7.70 m/s (Table S4).

High amounts of surface shear stress were present in most areas of the stoss slope during primary winds and greatest along the dune brink with a maximum value of 0.027 $kg \cdot m^{-1} \cdot s^{-2}$ with near-surface winds reaching approximately 17 m/s (Figures 2 and S6). Significant turbulent flow was generated on the lee side of the

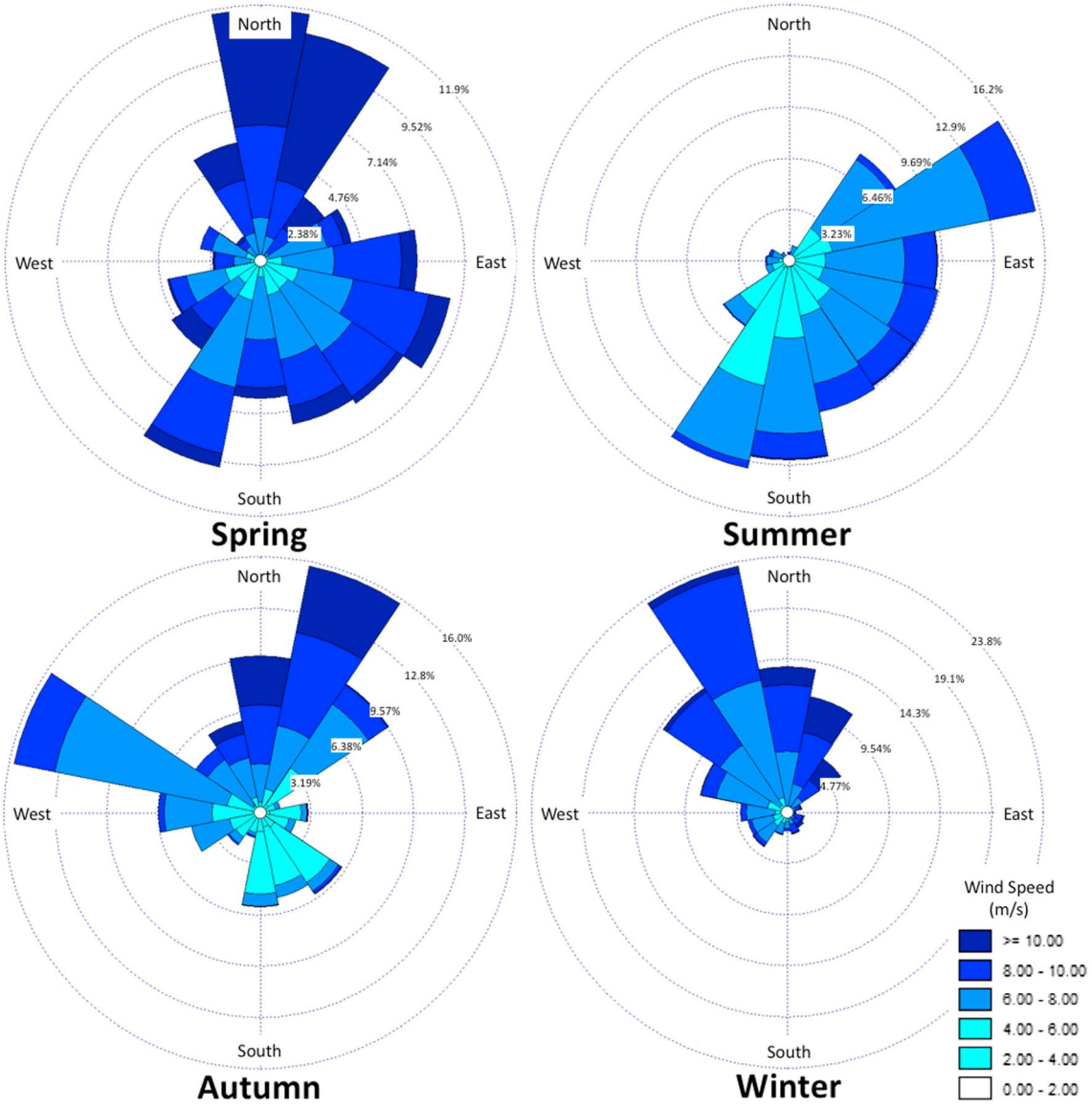

Figure 1. Rose diagrams showing seasonal Rover Environmental Monitoring Station wind data. Springtime winds are primarily from the north with secondary, reduced wind speeds from the south. Summer winds are weaker and originate from the southeast. Primary autumn winds are from the northeast with secondary winds from the west northwest and weaker tertiary winds from the southeast. Winter winds are primarily from the northwest. Some scatter in the data may be due to local topographic effects, but the general trends agree well with mesoscale models of Gale Crater.

Namib dune, where detached flow from the dune brink and complex helical flow was observed and a component of lateral airflow to the east accompanied the helices along the slipface.

Southerly winds flowed up the Namib slipface and over the brink, closely following the topography. These winds did not generate any complex flow, but elevated surface shear stress values were concentrated along the dune brink, having a maximum value of about 0.015 kg $\cdot$ m^{-1} $\cdot$ s^{-2}(Figures 2 and S7). The maximum near-surface wind velocities were approximately 13 m/s.

2.1.2. Summer (L_s 270°)

Wind direction during the summer was generally from the southeast but also ranged between NE to SSW (Figure 1). There was no secondary wind direction identified, and modeling results display southeast winds only. Average REMS wind velocity was approximately 6.46 m/s (Table S5). The maximum surface winds reached approximately 11 m/s, lower than spring winds originating from the same direction. With the lower surface wind velocities during the summer season, there was also a decrease in surface shear stress around

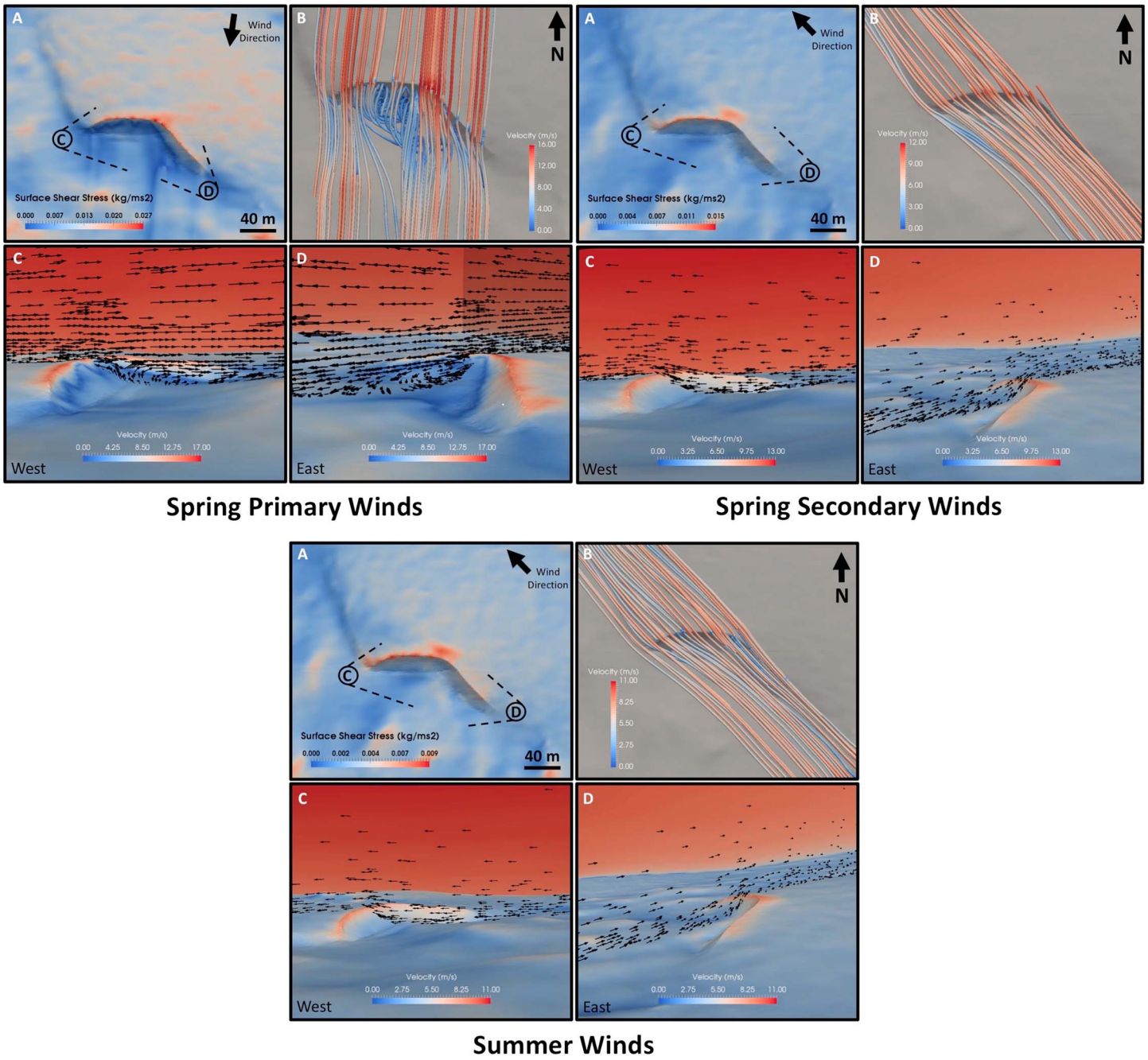

Figure 2. (a) Surface shear stress on the Namib dune including the viewer locations on the surface for panels c and d. (b) Velocity streamlines of spring and summer winds on the Namib dune with spring primary winds showing flow detachment from dune crest, and wind flow vectors as viewed from (c) the west flank and (d) the east flank of the dune, where the surface of panels c and d represent surface flow speed.

the Namib dune (Figure 2; S8). The more pronounced areas of surface shear stress occurred along the dune brink, reaching a maximum of approximately 0.009 kg · m^{-1} · s^{-2}. Modeling results showed no indication of complex airflow (Figure 2), similar to the southeast winds during spring.

2.1.3. Autumn (L_s 0°)

Autumn winds originated in three distinct directions during MY 33. The greatest magnitude winds (primary winds) were from the northeast, followed by secondary winds from the northwest and the lesser magnitude tertiary winds from the southeast (Figure 1). Winds fluctuated in all directions throughout the season, but the general shift in wind direction was toward the north near the end of the season.

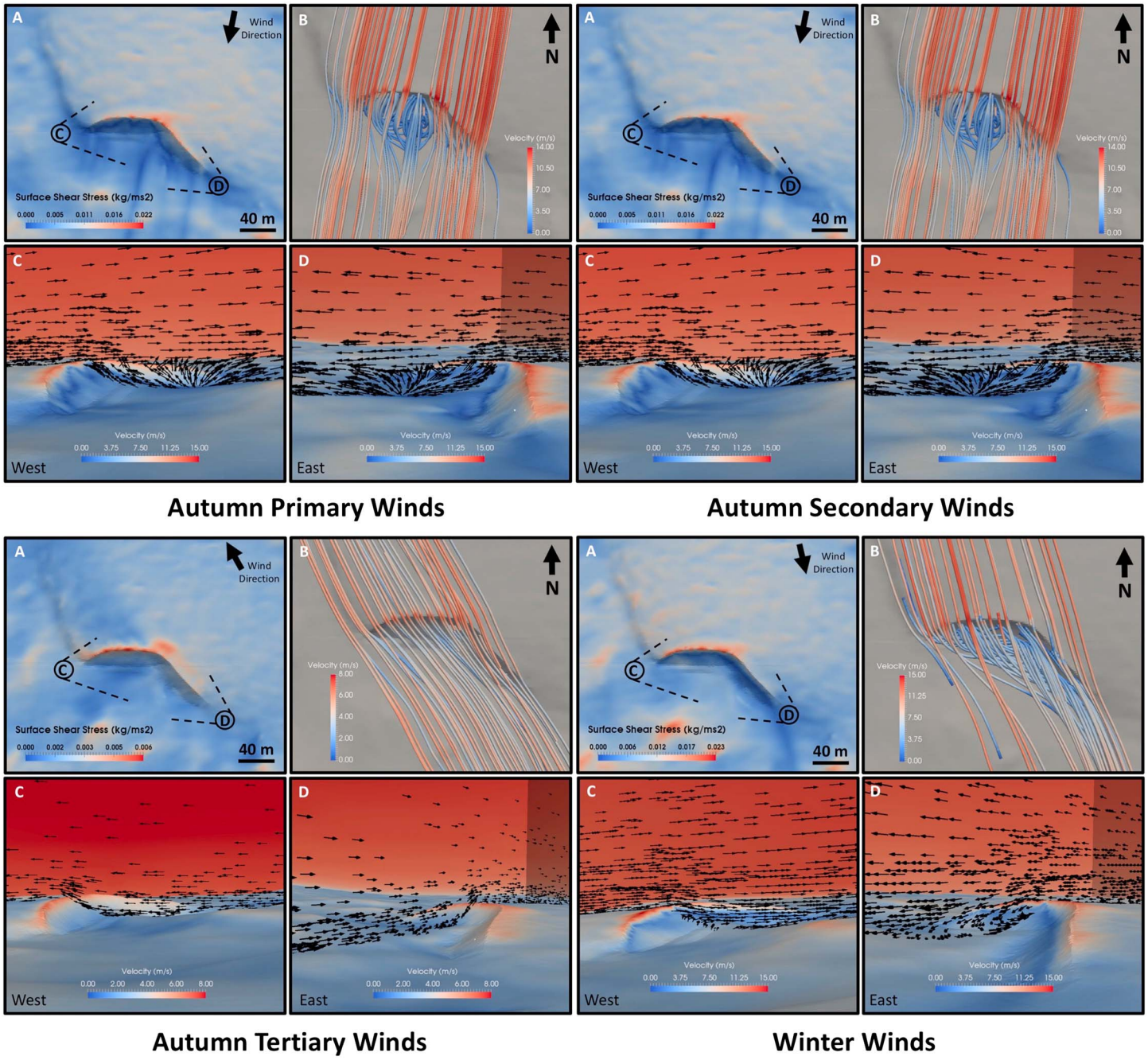

Figure 3. (a) Surface shear stress on the Namib dune including the viewer locations on the surface for panels C and D. (b) Velocity streamlines of autumn and winter winds on the Namib dune with autumn primary winds and winter winds showing flow detachment from dune crest, and wind flow vectors as viewed from (c) the west flank and (d) the opposite east flank of the dune, where the surface of panels c and d represent surface flow speed.

Greater values of surface shear stress were generated from the primary winds on the stoss compared to those generated from the southeast winds of spring and summer. The greatest amounts of surface shear stress were along the dune brink, reaching 0.022 kg $\cdot$ m^{-1} $\cdot$ s^{-2} (Figures 3 and S9) with near-surface wind velocities reaching 15 m/s. The average REMS wind speed of the primary wind direction was about 8.25 m/s (Table S4) and produced complex airflow on the lee side of the Namib dune (Figure 3). Compared to the spring northerly winds, the autumn northerly winds had a more eastern component and there was less lateral flow to the east from helices along the slipface. There was, however, a more pronounced backflow up the slipface slope when compared to spring (Figures 2 and 3).

The secondary autumn REMS wind speeds averaged about 6.74 m/s (Table S4) and originated from the northwest. Near-surface modeled wind speeds reached 12 m/s, and surface shear stress had the greatest affect along the western flank of Namib dune (Figure 3; S10) with a maximum value of about 0.013 kg · m^{-1} · s^{-2}.These winds did not produce any complex airflow, instead following the dune topography (Figure 3), similar to southeast winds.

The tertiary southeastern autumn winds had the lowest average REMS wind speed of 5.05 m/s (Table S4) and generated values of surface shear stress of about 0.006 kg · m^{-1} · s^{-2} (Figure 3; S11). Modeled near-surface winds reached a maximum of about 8 m/s and were concentrated along the Namib dune brink, but no complex airflow was observed.

2.1.4. Winter (L_s 90°)

Seasonal wind patterns during winter predominantly originated from the northwest. Winds from the southwest and southeast were not nearly as common in MY 33, and therefore, modeling was only conducted for northwest winds, which have the most influence on the eolian environment. The average REMS wind speed for the northwest winds was 8.06 m/s (Table S4). Maximum near-surface winds predicted by the model were approximately 15 m/s with a maximum surface shear stress value of about 0.023 kg · m^{-1} · s^{-2} along the dune brink (Figure 3; S12). Modeling revealed complex airflow on the lee side of the dune and included some flow steering around the dune with lateral flow to the east.

3. Discussion

3.1. Potential Seasonal Sediment Transport

The threshold of effective shear stress for sediment transport has been estimated to be 0.01 ± 0.0015 kg · m^{-1} · s^{-2} based on a study of Nili Patera grain saltation on Mars (Ayoub et al., 2014) and is used here to constrain when sediment transport occurs throughout the MY.

3.1.1. Spring Activity

Primary winds in the spring originating from the north occurred predominantly early in the season and were well over the shear stress threshold (Ayoub et al., 2014). These winds were perhaps the most influential of the year, capable of initiating grain saltation across the stoss slope with evidence of flow detachment at the dune crest and complex helices on the lee side of the dune (Figure 2) likely accompanied by grainfall. The secondary spring winds from the southeast may also initiate grain movement, focused along the Namib dune brink, with maximum surface shear stress values reaching just above the threshold at 0.015 kg · m^{-1} · s^{-2} (Figure 2). However, sediment movement may be largely constrained to a few isolated areas along the dune brink. In addition, the two wind directions from the north and southeast could form a divergence angle of approximately 90°, resulting in the cross-hatch ripple pattern observed on the stoss with an overall migration to the southwest throughout the spring season (e.g., Ewing et al., 2017; Silvestro et al., 2016).

3.1.2. Summer Activity

Average winds during MY 32 summer were primarily from the southeast, and maximum surface shear was just below the threshold value for grain movement at 0.009 kg · m^{-1} · s^{-2} (Figure 2) but within the error range (Ayoub et al., 2014), suggesting that some grain movement may have taken place. Since the modeling results are an average of the entire season, it is likely that there was periodic grain movement from gusts of wind or higher magnitude winds on certain days. Stoss ripple migration may have been temporarily halted or punctuated during this time with the dominating southeast winds continuing to rework the smaller stoss ripples orthogonal to the larger stoss ripples.

3.1.3. Autumn Activity

The greatest wind speeds in MY 33 autumn originated from the north and had the capacity to initiate sediment saltation on the stoss slope and along the dune brink with a maximum surface shear stress value of 0.022 kg · m^{-1} · s^{-2} (Figure 3). Flow separation occurred in the modeling results and may have been accompanied by grainfall and grainflow activity. Secondary winds during autumn were more westerly but also had the potential for sediment movement, especially along the dune brink, with surface shear stress reaching 0.013 kg · m^{-1} · s^{-2}. The western flank of the dune and parts of the western stoss slope may also have experienced sediment transport (Figure 3). Autumn southeast tertiary winds were the weakest of the season and likely did not initiate grain movement, even along the dune brink where shear stress barely reached 0.006 kg · m^{-1} · s^{-2} (Figure 3). The stoss ripples may be reactivated during autumn with the high

variability in wind direction throughout the season. In contrast to the spring season, ripples may be reworked by both northwestern winds and southeastern winds in conjunction with northeastern winds. This would result in an overall ripple migration to the southwest, similar to the spring season, but under a different wind regime (Ewing et al., 2017; Silvestro et al., 2016).

3.1.4. Winter Activity

Winter winds in MY 33 originated primarily from the northwest and generated surface shear stress values sufficient for sediment saltation. The maximum shear stress reached 0.023 $kg \cdot m^{-1} \cdot s^{-2}$, where elevated shear stress values were concentrated along the brink and the stoss slope (Figure 3). Winter airflow patterns also showed flow detachment at the dune brink and complex helical patterns on the lee side of the dune (Figure 3) potentially producing grainfall comparable to spring primary wind conditions. Since the winds are largely unidirectional during the winter, stoss ripple migration may once again cease during this season.

3.2. Implications for Slipface Activity

Slipface activity, such as that preserved on the Namib dune (Bridges et al., 2017; Cornwall, Bourke, et al., 2018; Ewing et al., 2017), requires large amounts of sediment to achieve localized slope over steepening near the brink, triggering a grainflow. It is through grainfall and multiple of grainflows that slipface advancement is achieved (e.g., Allen, 1970; Anderson, 1988; Bagnold, 1941; Hunter, 1977, 1985; Kok et al., 2012; McDonald & Anderson, 1995). The Namib slipface suggests that at some point(s) during the year, the slipface was very active despite the absence of eolian activity observed in late autumn by Curiosity (Bridges et al., 2017).

3.2.1. Northerly Winds

The magnitude and direction of winds during the Curiosity observation are characteristic of autumn secondary winds (Table S4 and Figure 3). The greater magnitude winds measured by REMs during this time (>5 m/s) generate surface shear stress values up to 0.013 $kg \cdot m^{-1} \cdot s^{-2}$ (Figure 3), sufficient for grain transport along the western flank and brink (Ayoub et al., 2014). Under westerly winds, large portions of the dune slipface are sheltered (Figure 3), and it is probable that from the perspective of the rover in front of the Namib dune, no activity could have been observed. Alternatively, observation could have taken place during quiescent days uncharacteristic of the seasonal average conditions. Curiosity's visit to the dunes coincided with some of the colder temperatures of the year, and it is possible that the dune sediment may have been indurated from seasonal frost (Bridges et al., 2017). During the nighttime, a few micrometers of frost can condense within porous spaces of the dune sand, potentially cementing the top layer of sand during the day (Martinez et al., 2016). If this process occurs during colder seasonal temperatures, the dune sediment may be immobilized during much of the autumn as well as winter seasons.

Based on CFD modeling results, there are a few times during the Martian year, such as early spring and winter, that may be more favorable to grainfall and slipface activity. Some of the seasonal wind patterns may also explain ripple formation around and on the slipface of the dune as well as the maintenance of the ladderback ripples on the stoss slope that require lower magnitude, opposing or oblique wind directions relative to the primary winds that facilitate dune migration to the south (Ewing et al., 2017). Northerly winds flowing over the stoss slope and encountering the dune brink between angles 40° to 90° are likely to generate grainfall, airflow separation, and complex three-dimensional vortices on the lee side of the dune (Eastwood et al., 2012; Ewing et al., 2010; Ewing et al., 2017), which is consistent with modeling results. Flow separation and the formation of three-dimensional helices occurred during early spring, autumn and the winter season (Figures 2 and 4). It is possible that the remnants of slipface activity imaged by Curiosity occurred earlier in the autumn season or even earlier in the year during spring.

Spring exhibited the highest magnitude northerly winds early in the season and is likely a time of significant slipface activity and dune advancement. There is also likely lateral transport to the east due to the helical wind patterns along the lee slope of the dune (Figure 2), which was detected by Curiosity in autumn (Bridges et al., 2017; Ewing et al., 2017). Depending on the incidence angle of the wind on the brink line, the magnitude of this eastward transport would vary, where northwest winds would generate much stronger lateral airflow along the lee slope than more northerly or northeasterly winds (Figures 2 and 4). This lateral transport can also be augmented by flow steering around the western flank of the Namib dune (Figure 3).

3.2.2. Southerly Winds

Secondary springtime winds and, to a lesser extent, summer winds and autumn tertiary winds (Figures 2 and 4) may erase slipface features and rework the dune brink by reversing sediment transport down the stoss

slope. Southerly winds may also significantly influence the stoss slope, maintaining the ladderback ripple pattern observed in Curiosity Mastcam images (Ewing et al., 2017). In addition, the seasonal southerly winds with a more easterly component with sufficient wind speed to generate sediment transport may activate the secondary slipface along the western flank of the dune (Ewing et al., 2017). Autumn secondary winds were more westerly (Figure 3) and had the potential to redistribute sediment and rework the brink line. These more westerly winds may be highly influential in forming the ripples that cover the Namib slipface (Bridges et al., 2017; Cornwall, Bourke, et al., 2018; Ewing et al., 2017) as well as reworking the western flank and transporting sediment to the east.

3.3. Overall Dune Migration Patterns

The Bagnold dunes are migrating ~0.2 m/MY with ripples migrating at a quicker rate of ~0.33 m/MY (Silvestro et al., 2013). The Namib dune was specifically examined to detect change using HiRISE images during MY 33, which overlapped with the time of Curiosity's visit to the dunes, and was observed to advance ~0.4 m (Bridges et al., 2017). The stoss ripples moved more rapidly and could not be confidently tracked. Overall sediment movement in the dune field showed that the most active seasons in MY 33 for migration were during spring to summer (Bridges et al., 2017).

Despite the favorable wind direction and magnitude in the autumn and winter seasons, the Namib dune sediment experienced very little displacement according to HiRISE image monitoring. This may be due to frost condensation in between sand grains and subsequent induration of the dune sediment (Bridges et al., 2017; Martinez et al., 2016). However, an extremely low volatile content was measured near the dune (e.g., Ehlmann et al., 2017), making this hypothesis unlikely. The lack of significant slipface advancement during any other season besides spring and summer in MY 33 may suggest that the preserved slipface activity formed earlier in the Martian year when winds were more conducive to grainfall. However, the lower magnitude summer southerly winds would have little influence on grainflow formation. Therefore, the grainflows on the slipface may have occurred earlier in autumn over a few days but not prolonged enough to result in detectable slipface advancement.

The large stoss ripple crestlines on the dune are oriented NW and NE and intersect the dune brink obliquely along the horns and transversely in the center (Lapotre et al., 2016; Silvestro et al., 2013). These ripples may be most active during the spring and autumn seasons when differing wind regimes would result in the crosshatch pattern of the ripples and drive migration to the southwest. As the ripples migrate, significant amounts of sediment may be introduced to the slope (Cornwall, Bourke, et al., 2018; Ewing et al., 2017), augmenting slipface advancement. With the unidirectional winter winds, stoss ripple migration may cease, alternatively explaining why dune migration rates are not as rapid as the spring season.

The migration of stoss ripples may prolong grainflow beyond the spring and autumn seasons by creating localized over steepening on the slipface from sediment deposition. However, without grainfall, this mechanism for grainflow is likely short-lived until higher magnitude winds can generate grainfall or redistribute sediment, restoring the slipface (e.g., Allen, 1970; Anderson, 1988; Bagnold, 1941; Cornwall, Jackson, et al., 2018; Hunter, 1977; Hunter, 1985; Kok et al., 2012; McDonald & Anderson, 1995). Some of the grainflows imaged by Curiosity during late autumn (Bridges et al., 2017), may be a product of such activity. In addition, when winds are blowing from the south, it is possible that the dune brink may be smoothed and sediment transport may be reversed, as indicated by the elevated surface shear stress values in the model output. However, indications of brink smoothing have not been evident in HiRISE or Curiosity rover images.

4. Conclusion

Dune length scale CFD modeling has provided the necessary means to better understand the interaction between local wind regime and eolian bedform response. Modeling results show a detailed spatial pattern of seasonal wind turbulence patterns and intensity of airflow that offers critical insights into seasonal sediment transportation and implications for sediment flux that cannot be resolved by coarser mesoscale modeling or derived by ripple mapping studies. In addition, there are flow structures present on dunes that cannot be studied by any other means other than CFD modeling such as flow detachment from the dune brink. These new insights are presented herein for the Namib dune throughout the Martian year, highlighting seasons that are more conducive to dune and ripple migration.

Acknowledgments
We would like to give thanks to Colin Anderson for assistance in technical support and OpenFOAM trouble shooting and Chris McGonigle for edits and suggestions of the manuscript. Also many thanks to the reviewers of this paper, Simone Silvestro and an anonymous reviewer for their helpful comments and revisions. This research was funded by the Vice Chancellor's Research Scholarship, University of Ulster, and Natural Environment Research Council grant NE/F019483/1. M. C. B.'s contribution was supported in part by EU FP7 CIG 618892. The Mars Science Laboratory Curiosity rover mission data used in this study is freely accessible on NASA's Planetary Data System (PDS) archives website.

References

Allen, J. (1970). The avalanching of granular solids on dune and similar slopes. *Journal of Geology*, *78*(3), 326–351. https://doi.org/10.1086/627520

Anderson, R. (1988). The pattern of grainfall deposition in the lee of aeolian dunes. *Sedimentology*, *35*(2), 175–188. https://doi.org/10.1111/j.1365-3091.1988.tb00943.x

Ayoub, F., Avouac, J.-P., Newman, C. E., Richardson, M. I., Lucas, A., Leprince, S., & et al. (2014). Threshold for sand mobility on Mars calibrated from seasonal variations of sand flux. *Nature Communications*, *5*(1). https://doi.org/10.1038/ncomms6096

Bagnold, R. (1941). The physics of blown sand and desert dunes, p. 265, Methuen, London.

Bridges, N. T., & Ehlmann, B. H. (2017). The Mars Science Laboratory (MSL) Bagnold Dunes Campaign, Phase I: Overview and introduction to the special issue. *Journal of Geophysical Research: Planets*, *123*, 3–19. https://doi.org/10.1002/2017JE005401

Bridges, N. T., Sullivan, R., Newman, C. E., Navarro, S., van Beek, J., Ewing, R. C., et al. (2017). Martian aeolian activity at the Bagnold Dunes, Gale Crater: The view from the surface and orbit. *Journal of Geophysical Research: Planets*, *122*, 2544–2573. https://doi.org/10.1002/2017JE005324

Cornwall, C., Bourke, M. C., Jackson, D. W. T., & Cooper, J. A. G. (2018). Aeolian slipface dynamics and grainflow morphologies on Earth and Mars. *Icarus*, *314*, 311–326. https://doi.org/10.1016/j.icarus.2018.05.033

Cornwall, C., Jackson, D. W. T., Bourke, M. C., & Cooper, J. A. G. (2018). Morphometric analysis of slipface processes of an aeolian dune: Implications for grain-flow dynamics. *Sedimentology*. https://doi.org/10.1111/sed.12456

Crane Company (1988). Flow through valves, fittings and pipe, Technical Paper No. 410, Joliet, I11:Crane Company.

Day, M., & Kocurek, G. (2016). Observations of an aeolian landscape: From surface to orbit in Gale Crater. *Icarus*, *280*, 37–71. https://doi.org/10.1016/j.icarus.2015.09.042

Delgado-Fernandez, I., Jackson, D. W. T., Cooper, J. A. G., Baas, A. C. W., Beyers, J. H. M., & Lynch, K. (2013). Field characterization of three-dimensional lee-side airflow patterns under offshore winds at a beach-dune system. *Journal of Geophysical Research: Earth Surface*, *118*, 706–721. https://doi.org/10.1002/jgrf.20036

Eastwood, E. N., Kocurek, G., Mohrig, D., & Swanson, T. (2012). Methodology for reconstructing wind direction, wind speed, and duration of wind events from aeolian cross-strata. *Journal of Geophysical Research*, *117*, F03035. https://doi.org/10.1029/2012JF002368

Ehlmann, B. L., Edgett, K. S., Sutter, B., Achilles, C. N., Litvak, M. L., Lapotre, M. G. A., et al. (2017). Chemistry, mineralogy, and grain properties at Namib and High Dunes, Bagnold Dune Field, Gale Crater, Mars: A synthesis of Curiosity Rover observations. *Journal of Geophysical Research: Planets*, *122*, 2510–2543. https://doi.org/10.1002/2017JE005267

Ewing, R. C., Lapotre, M. G. A., Lewis, K. W., Day, M., Stein, N., Rubin, D. M., et al. (2017). Sedimentary structures of the Bagnold Dunes: Implications for eolian rock record of Mars. *Journal of Geophysical Research: Planets*, *122*, 2544–2573. https://doi.org/10.1002/2017JE005324

Ewing, R. C., Peyret, A. P. B., Kokurek, G., & Bourke, M. C. (2010). Dune field pattern formation and recent transporting winds in the Olympia Undae Dune Field, north polar region of Mars. *Journal of Geophysical Research*, *115*, E08005. https://doi.org/10.1029/2009JE003526

Fenton, L. K., & Richardson, M. I. (2001). Martian surface winds: Insensitivity to orbital changes and implications for aeolian processes. *Journal of Geophysical Research*, *106*, 32,885–32,902. https://doi.org/10.1029/2000JE001407

Fenton, L. K., Toigo, A. D., & Richardson, M. I. (2005). Aeolian processes in Proctor Crater on Mars: Mesoscale modelling of dune-forming winds. *Journal of Geophysical Research*, *110*, E06005. https://doi.org/10.1029/2004JE002309

Greeley, R., Arvidson, R. E., Barlett, P. W., Blaney, D., Cabrol, N. A., Christensen, P. R., et al. (2006). Gusev crater: Wind-related features and processes observed by the Mars Exploration Rover Spirit. *Journal of Geophysical Research*, *111*, E02S09. https://doi.org/10.1029/2005JE002491

Greeley, R., & Iversen, J. D. (1985). *Wind as a Geological Process on Earth, Mars, Venus and Titan. Cambridge Planetary Science Series* (Vol. 40). Cambridge: Cambridge University Press.

Greeley, R., Leach, R., White, B., Iversen, J., & Pollack, J. (1980). Threshold windspeeds for sand on Mars: Wind tunnel simulations. *Geophysical Research Letters*, *7*, 121–124. https://doi.org/10.1029/GL007i002p00121

Greeley, R., Skypeck, A., & Pollack, J. B. (1993). Martian aeolian features and deposits: Comparisons with general circulation model results. *Journal of Geophysical Research*, *98*, 3183–3196. https://doi.org/10.1029/92JE02580

Haberle, R. M., Pollack, J. B., Barnes, J. R., Zurek, R. W., Leovy, C. B., Murphy, J. R., et al. (1993). Mars atmospheric dynamics as simulated by the NASA Ames general circulation model, 1. The zonal mean circulation. *Journal of Geophysical Research*, 3093–3123. https://doi.org/10.1029/92JE02946

Hayward, R. K., Fenton, L. K., Tanaka, K. L., Titus, T. N., Colaprete, A., & Christensen, P. R. (2008). Aeolian features as ground truth for atmospheric modelling on Mars, in Third International Workshop on the Mars Atmosphere: Modelling and Observations, *LPI Contrib*. 1447, p. 9033.

Hayward, R. K., Mullins, K. F., Fenton, L. K., Hare, T. M., Titus, T. N., Bourke, M. C., et al. (2007). Mars Global Digital Dune Database and initial science results. *Journal of Geophysical Research*, *112*, E11007. https://doi.org/10.1029/2007JE002943

Hayward, R. K., Titus, T. N., Michaels, T. I., Fenton, L. K., Colaprete, A., & Christensen, P. R. (2009). Aeolian dunes as ground truth for atmospheric modelling on Mars. *Journal of Geophysical Research*, *114*, E11012. https://doi.org/10.1029/2009JE003428

Hebrard, E., Listowski, C., Coll, P., Marticorena, B., Bergametti, G., Maattanen, A., et al. (2012). An aerodynamic roughness length map derived from extended Martian rock abundance. *Journal of Geophysical Research*, *117*, E04008. https://doi.org/10.1029/2011JE003942

Hecht, M. H. (2002). Metastability of liquid water on Mars. *Icarus*, *156*(2), 373–386. https://doi.org/10.1006/icar.2001.6794

Hobbs, S. W., Paull, D. J., & Bourke, M. C. (2010). Aeolian processes and dune morphology in Gale Crater. *Icarus*, *210*(1), 102–115. https://doi.org/10.1016/j.icarus.2010.06.006

Hourdin, F., & Forget, F. (1995). The sensitivity of the Martian surface pressure and atmospheric mass budget to various parameters: A comparison between numerical simulations and Viking observations. *Journal of Geophysical Research*, *100*, 5501–5523. https://doi.org/10.1029/94JE03079

Hunter, R. (1985). A kinematic model for the structure of lee-side deposits. *Sedimentology*, *32*(3), 409–422. https://doi.org/10.1111/j.1365-3091.1985.tb00520.x

Hunter, R. E. (1977). Basic types of stratification in small eolian dunes. *Sedimentology*, *24*(3), 361–387. https://doi.org/10.1111/j.1365-3091.1977.tb00128.x

Jackson, D. W., Bourke, M. C., & Smyth, T. A. (2015). The dune effect on sand-transporting winds on Mars. *Nature Communications*, *6*(1), 8796. https://doi.org/10.1038/ncomms9796

Jackson, D. W. T., Beyers, J. H. M., Lynch, K., Cooper, J. A. G., Baas, A. C. W., & Delgado-Fernandez, I. (2011). Investigation of three-dimensional wind flow behaviour over coastal dune morphology under offshore winds using computational fluid dynamics (CFD) and ultrasonic anemometry. *Earth Surface Processes and Landforms*, *36*(8), 1113–1124. https://doi.org/10.1002/esp.2139

Jackson, D. W. T., Beyers, M., Delgado-Fernandez, I., Baas, A. C. W., Cooper, J. A. G., & Lynch, K. (2013). Airflow reversal and alternating corkscrew vortices in foredune wake zones during perpendicular and oblique offshore winds. *Geomorphology*, *187*, 86–93. https://doi.org/10.1016/j.geomorph.2012.12.037

Kok, J. F. (2010a). An improved parameterization of wind-blown sand flux on Mars that includes the effect of hysteresis. *Geophysical Research Letters*, *37*, L12202. https://doi.org/10.1029/2010GL043646

Kok, J. F. (2010b). Difference in wind speeds required for initial versus continuation of sand transport on Mars: Implications for dunes and dust storms. *Physical Review Letters*, *104*, 074502. https://doi.org/10.1103/PhysRevLett.104.074502

Kok, J. F., Parteli, E. J., Michaels, T. I., & Karam, D. B. (2012). The physics of wind-blown sand and dust. *Reports on Progress in Physics*, *75*(10), 106901. https://doi.org/10.1088/0034-4885/75/10/106901

Kok, J. F., & Renno, N. O. (2009). A comprehensive numerical model of steady state saltation (COMSALT). *Journal of Geophysical Research*, *114*, D17204. https://doi.org/10.1029/2009JD011702

Lapotre, M., Ewing, R. C., Lamb, M. P., Fischer, W. W., Grotzinger, J. P., & Rubin, D. M. (2016). Large wind ripples on Mars: A record of atmospheric evolution. *Science*, *353*(6294), 55–58. https://doi.org/10.1126/science.aaf3206

Lee, P., & Thomas, P. C. (1995). Longitudinal dunes on Mars: Relation to current wind regimes. *Journal of Geophysical Research*, *100*, 5381–5395. https://doi.org/10.1029/95JE00225

Leovy, C., & Mintz, Y. (1969). Numerical simulation of the atmospheric circulation and climate of Mars. *Journal of Atmospheric Science*, *26*(6), 1167–1190. https://doi.org/10.1175/1520-0469(1969)026<1167:NSOTAC>2.0.CO;2

Martinez, G. M., Fischer, E., Rennó, N. O., Sebastián, E., Kemppinen, O., Bridges, N., et al. (2016). Likely frost events at Gale crater: Analysis from MSL/REMS measurements. *Icarus*, *280*, 93–102. https://doi.org/10.1016/j.icarus.2015.12.004

McDonald, R., & Anderson, R. (1995). Experimental verification of aeolian saltation and lee side deposition models. *Sedimentology*, *42*(1), 39–56. https://doi.org/10.1111/j.1365-3091.1995.tb01270.x

Newman, C., Gomez-Elvira, J., Marin, M., Navarro, S., Torres, J., Richardson, M. I., et al. (2017). Winds measured by the Rover Environmental Monitoring Station (REMS) during the Mars Science Laboratory (MSL) rover's Bagnold Dunes Campaign and comparison with numerical modelling using MarsWRF. *Icarus*, *291*, 203–231. https://doi.org/10.1016/j.icarus.2016.12.016

Nield, J. M., Wiggs, G. F., Baddock, M. C., & Hipondoka, M. H. (2017). Coupling leeside grainfall to avalanche characteristics in aeolian dune dynamics. *Geology*, *45*(3), 271–274.

Pla-Garcia, J., Rafkin, S. C. R., Kahre, M., Gomez-Elvira, J., Hamilton, V. E., Navarro, S., et al. (2016). The meteorology of Gale Crater as determined from rover environmental monitoring station observations and numerical modelling. Part I: Comparison of model simulations with observations. *Icarus*, *280*, 103–113.

Rafkin, S. C. R., Haberle, R. M., & Michaels, T. I. (2001). The Mars Regional Atmospheric Modelling System: Model description and selected simulations. *Icarus*, *151*(2), 228–256. https://doi.org/10.1006/icar.2001.6605

Rafkin, S. R. C., Pla-Garcia, J., Kahre, M., Gomez-Elvira, J., Hamilton, V. E., Marin, M., et al. (2016). The meteorology of Gale Crater as determined from rover environmental monitoring station observations and numerical modelling. Part II: Interpretation. *Icarus*, *280*, 114–138. https://doi.org/10.1016/j.icarus.2016.01.031

Richards, P. J., & Norris, S. E. (2011). Appropriate boundary conditions for computational wind engineering models revisited. *Journal of Wind Engineering and Industrial Aerodynamics*, *99*(4), 257–266. https://doi.org/10.1016/j.jweia.2010.12.008

Richardson, M. I., Toigo, A. D., & Newman, C. E. (2007). PlanetWRF: A general purpose, local to global numerical model for planetary atmospheric and climate dynamics. *Journal of Geophysical Research*, *112*, E09001. https://doi.org/10.1029/2006JE002825

Schatz, V., & Herrmann, H. J. (2006). Flow separation in the lee side of transverse dunes: A numerical investigation. *Geomorphology*, *81*(1-2), 207–216. https://doi.org/10.1016/j.geomorph.2006.04.009

Silvestro, S., Vaz, D. A., Ewing, R. C., Rossi, A. P., Fenton, L. K., Michaels, T. I., et al. (2013). Pervasive aeolian activity along rover Curiosity's traverse in Gale Crater, Mars. *Geology*, *41*(4), 483–486. https://doi.org/10.1130/G34162.1

Silvestro, S., Vaz, D. A., Yizhaq, H., & Esposito, F. (2016). Dune-like dynamic of Martian aeolian large ripples. *Geophysical Research Letters*, *43*, 8384–8389. https://doi.org/10.1002/2016GL070014

Smyth, T. A. G., Jackson, D. W. T., & Cooper, J. A. G. (2011). Computational fluid dynamic modelling of three-dimensional airflow over dune blowouts. *Journal of Coastal Research*, *64*, 314–318.

Smyth, T. A. G., Jackson, D. W. T., & Cooper, J. A. G. (2012). High resolution measured and modelled three-dimensional airflow over a coastal bowl blowout. *Geomorphology*, *177*, 62–73.

Smyth, T. A. G., Jackson, D. W. T., & Cooper, J. A. G. (2013). Three dimensional airflow patterns within a coastal trough–bowl blowout during fresh breeze to hurricane force winds. *Aeolian Research*, *9*, 111–123.

Spiga, A., & Forget, F. (2009). A new model to simulate the Martian mesoscale and microscale atmospheric circulation: Validation and first results. *Journal of Geophysical Research*, *114*, E02009. https://doi.org/10.1029/2008JE003242

Sutton, S. L. F., McKenna Neuman, C., & Nickling, W. (2013). Lee slope sediment processes leading to avalanche initiation on an aeolian dune. *Journal of Geophysical Research: Earth Surface*, *118*, 1754–1766. https://doi.org/10.1002/jgrf.20131

Toigo, A. D., & Richardson, M. I. (2002). A mesoscale model for the Martian atmosphere. *Journal of Geophysical Research*, *107*(E7), 5049. https://doi.org/10.1029/2000JE001489

Tyler, D., Barnes, J. R., & Haberle, R. M. (2002). Simulation of surface meteorology at the Pathfinder and VL1 sites using a Mars mesoscale model. *Journal of Geophysical Research*, *107*(E4), 5018. https://doi.org/10.1029/2001JE001618

Wiggs, G. F. S., & Weaver, C. M. (2012a). Turbulent flow structures and aeolian sediment transport over a barchan sand dune. *Geophysical Research Letters*, *39*, L05404. https://doi.org/10.1029/2012GL050847